Density profiles of fluids confined in spherical cages



1996 J. Phys.: Condens. Matter 8 959

(http://iopscience.iop.org/0953-8984/8/8/007)

J. Phys.: Condens. Matter **8** (1996) 959–967. Printed in the UK

# Density profiles of fluids confined in spherical cages

Soon-Chul Kim†

Department of Physics, Andong National University, Andong, 760-749, Korea

Received 9 August 1995, in final form 30 October 1995

**Abstract.** Two different free-energy functional approximations, which are the hybrid-weighted-density approximation (HWDA) and global hybrid-weighted-density approximation (GHWDA) proposed by Kim, Calleja and Rickayzen, have been applied in the study of the density profiles of hard-sphere and Lennard-Jones fluids confined in spherical cages. For the density profiles of hard-sphere fluid, both the HWDA and the GHWDA at lower density are in a good agreement with the computer simulations. However, at higher density $\rho\sigma^3 = 0.75$ the GHWDA shows better agreement than the HWDA and compares well with the computer simulations. For the Lennard-Jones fluid, the density-functional perturbation theory (DFPT) based on the second-order perturbation theory of the uniform liquid has been examined. The calculated results show that the DFPT compares well with computer simulations although the agreement deteriorates slightly as the temperature of the Lennard-Jones fluid is reduced.

## 1. Introduction

In a recent paper [1], we have proposed the hybrid-weighted-density approximation (HWDA) and global hybrid-weighted-density approximation (GHWDA). In one of the approximations the weighted function is constructed to satisfy the same homogeneous properties as the local weighted-density approximation (LWDA) proposed by Tarazona (see [2, 3, 4]); in the other, the weighting function is constructed to agree with that of Leidl and Wagner [5] for the homogeneous fluid. We have derived the free-energy functional approximations, which are mathematically less intensive forms, from two hybrid-weighted-density approximations. We have applied the free-energy functional approximations in investigating the structural properties of nonuniform hard-sphere fluid restricted by hard and permeable walls. For the hard-sphere fluid confined between planar hard walls, the results for the HWDA are almost indistinguishable from those for the LWDA of Tarazona, although at the highest density investigated the HWDA is in closer agreement with simulation. When the walls are permeable, the HWDA produced profiles are again almost indistinguishable from the due to Tarazona's theory except near the centre of a permeable wall. However, although we did not publish the results for the GHWDA for the density profiles of hard-sphere fluid restricted by hard walls and permeable walls [6], the comparisons with those of the HWDA show that for the hard-sphere fluid confined between planar hard walls the GHWDA is better than for the HWDA compared with the computer simulation, whereas for the hard-sphere fluid confined by permeable walls the HWDA is better than the GHWDA for a wide range of parameters. These results suggest that the structural properties of hard-sphere fluid depend on the geometrical features of walls as well as the wall potentials. Thus, we have applied the HWDA and GHWDA in studying the structural properties of

† E-mail address: sckim@anu.andong.ac.kr

0953-8984/96/080959+09$19.50  

hard-sphere and Lennard-Jones fluids confined in spherical cages because (i) less intensive studies have been reported for the spherical cages rather than slit or cylindrical pores [7] and (ii) the free-energy functional approximation for the hard-sphere fluid can be used as a reference system for the perturbative analysis of Lennard-Jones fluid. For the Lennard-Jones fluid, the density-functional perturbation theory (DFPT) [8, 9, 10] based on the second-order perturbation theory of the uniform liquid has been used.

In section 2, we will apply two different free-energy functional approximations, the HWDA and GHWDA, to predict the density profiles of hard-sphere fluid confined in a spherical cage with a hard structureless wall. We will compare our results with other model approximations and computer simulations. In section 3, we will use the DFPT to investigate the structural behaviour of Lennard-Jones fluid confined in a spherical cage. A brief discussion on the strengths and weakness of the HWDA and GHWDA in future applications are included in the final section.

## 2. Density profiles of hard-sphere fluid

For the system of hard-sphere fluid confined in a spherical hard-wall cage of radius $R$, the resulting density profile equation [1] is given by

$$\rho(r) = \begin{cases} \rho_b \exp[c^{(1)}(r;[\rho]) - c^{(1)}(\rho_b)] & r < R \\ 0 & r > R \end{cases} \tag{1}$$

where $\rho_b$ is the bulk density of hard-sphere fluid, and $c^{(1)}(\rho_b)$ and $c^{(1)}(r;[\rho])$ are the one-particle direct correlation functions of hard-sphere fluid in the homogeneous and inhomogeneous states, respectively. The one-particle direct correlation function $c^{(1)}(\boldsymbol{r}:[\rho])$ appearing in equation (1) is defined as

$$c^{(1)}(\boldsymbol{r}:[\rho]) = -\frac{\delta\beta F[\rho]_{ex}}{\delta\rho(\boldsymbol{r})} \tag{2}$$

where $\beta = 1/k_B T$, and $F[\rho]_{ex}$ is the excess free energy arising from the particle interaction. For the HWDA and GHWDA [1], $c^{(1)}(r;[\rho])$ is given by

$$c^{(1)}(\boldsymbol{r};[\rho]) = -\beta f(\bar{\rho}(\boldsymbol{r})) - \beta \int \mathrm{d}\boldsymbol{s}\, \rho(\boldsymbol{s}) f'(\bar{\rho}(\boldsymbol{s})) \frac{\delta\bar{\rho}(\boldsymbol{s})}{\delta\rho(\boldsymbol{r})} \tag{3}$$

and for $c^{(1)}(\rho_b)$

$$c^{(1)}(\rho_b) = -\beta f(\rho_b) - \beta\rho f'(\rho_b) \tag{4}$$

where

$$\frac{\delta\bar{\rho}(\boldsymbol{s})}{\delta\rho(\boldsymbol{r})} = \omega(\boldsymbol{r}-\boldsymbol{s}, \tilde{\rho}(\boldsymbol{s})) + \omega(\boldsymbol{r}-\boldsymbol{s}, \rho) \int \mathrm{d}\boldsymbol{t}\, \rho(\boldsymbol{t}) \omega'(\boldsymbol{s}-\boldsymbol{t}, \tilde{\rho}(\boldsymbol{s})). \tag{5}$$

The density profiles are obtained by the numerical interaction between the old density profiles on the right-hand side and the new one on the left-hand side in equation (1). In applying equation (1), the excess free energy per particle of hard-sphere fluid, $f(\rho)$, is taken from the quasi-exact Carnahan–Starling equation of state [11]:

$$\beta f(\rho) = \frac{\eta(4-3\eta)}{(1-\eta)^2} \tag{6}$$

where $\eta = \pi\rho\sigma^3/6$ and $\sigma$ is the hard-sphere diameter.

In this case, two densities, $\rho_b\sigma^3 = 0.62$ with $N = 277$ and $\rho_b\sigma^3 = 0.75$ with $N = 342$, are investigated for the density profiles of hard-sphere fluid confined in spherical hard-wall

cages with $R = 4.5\sigma$, where $N$ is the total number of particles in the spherical cage. The resulting density profiles for the confined hard-sphere fluid are displayed in figures 1 and 2, and compared with the results of computer simulations [7]. As we can see in figure 1, the calculated results for the HWDA and the GHWDA for the lower density of $\rho_b\sigma^3 = 0.62$ are in excellent agreement with those obtained from the computer simulations. However, for the higher density of $\rho_b\sigma^3 = 0.75$, the GHWDA is well reproduced qualitatively and quantitatively compared with the computer simulations, whereas for the HWDA the position of the first peak is slightly shifted and the first oscillation is slightly underestimated. In particular, the hard-sphere oscillatory structures of HWDA near the centre of a spherical cage ($r = 0$) show different behaviours compared with those of the GHWDA and the computer simulations; the density at $r = 0$ is greater than that of the next peak and is well above 1. This effect near the centre can be seen in the LWDA of Tarazona although the density at $r = 0$ is slightly lower than that for the GHWDA [12]. Actually, we can expect this effect when the radius $R$ is very small and the density $\rho_b\sigma^3$ is high. However, $R = 4.5\sigma$ is not big and $\rho_b\sigma^3 = 0.75$ is not high compared with the freezing density of hard-sphere fluid $\rho_b\sigma^3 = 0.94$ [13]. This is what one would expect. In fact, the statistics in the computer simulations are not good near the centre of a spherical cage because of the small number of particles near the centre in the simulations. Nevertheless, the simulation density profiles also appear to be tending to the bulk density at the centre. It is very difficult to understand the density behaviour near the centre on physical grounds as well as that of the LWDA of Tarazona. Thus, we can conclude here that the GHWDA, compared with the HWDA, describes the structural properties of hard-sphere fluid well.

## 3. Density profiles of Lennard-Jones fluid

We consider the density profiles of Lennard-Jones fluid confined in a spherical cage. The excess free energy $F[\rho]_{ex}$ arising from the particle interaction can be generally written as [14]

$$F[\rho]_{ex} = \tfrac{1}{2}\int \mathrm{d}\boldsymbol{r}\,\rho(\boldsymbol{r})\int \mathrm{d}\boldsymbol{s}\,\rho(\boldsymbol{s})u(\boldsymbol{r}-\boldsymbol{s})\int_0^1 \mathrm{d}\lambda\, g(\boldsymbol{r},\boldsymbol{s};[\lambda\rho]) \tag{7}$$

where $\lambda$ is the charging parameter, $u(\boldsymbol{r})$ the intermolecular potential of fluids, and $g(\boldsymbol{r};[\rho])$ the pair correlation function of fluids. For the Lennard-Jones fluid, the intermolecular potential $u(\boldsymbol{r})$ is given by

$$u(r) = 4\epsilon\left[\left(\frac{\sigma}{r}\right)^{12} - \left(\frac{\sigma}{r}\right)^{6}\right] \tag{8}$$

where $\epsilon$ and $\sigma$ are the parameters of interaction strength and interaction range respectively. Since little is known about the pair correlation function $g(\boldsymbol{r};[\rho])$ for the Lennard-Jones potentials, we use the perturbation theory for calculating the excess free energy, equation (7). For this, we divide the excess free energy $F[\rho]_{ex}$ into repulsive and attractive contributions:

$$F[\rho]_{ex} = F^{rep}[\rho] + F^{att}[\rho]. \tag{9}$$

Then, we can also decompose the Lennard-Jones potential into repulsive and attractive parts as follows:

$$u^{rep}(r) = \begin{cases} u(r) & \text{for } r < \sigma \\ 0 & \text{for } r > \sigma \end{cases} \tag{10}$$

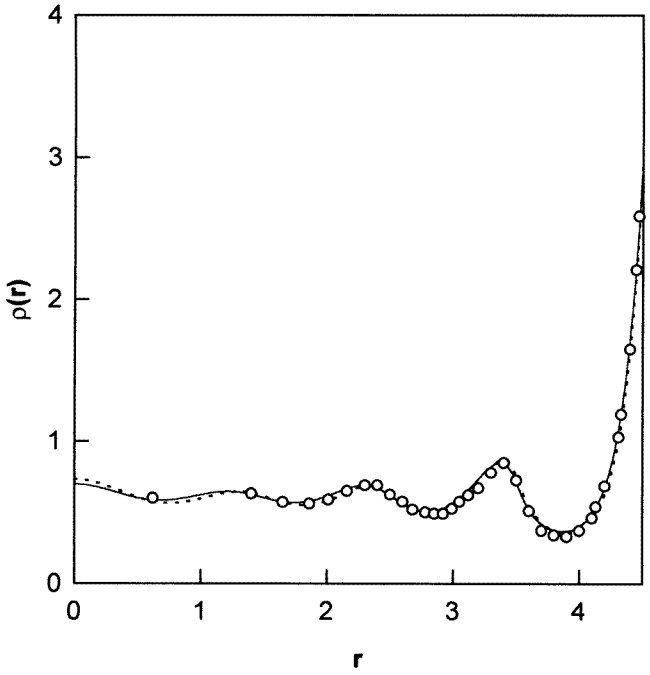


**Figure 1.** Density profiles of hard-sphere liquid confined in a spherical cage with a hard structure wall ($\rho_b\sigma^3 = 0.62$). The open circles are from the computer simulations [7]. The solid and dotted lines correspond to the HWDA and GHWDA, respectively.

and

$$u^{att}(r) = \begin{cases} 0 & \text{for } r < \sigma \\ u(r) & \text{for } r > \sigma. \end{cases} \tag{11}$$

In the perturbation theory of classical fluids, the repulsive part $F^{rep}[\rho]$ is subsequently represented by the hard-sphere contribution, whereas the attractive contribution $F^{att}[\rho]$ is treated as the perturbation term. Since the free energy $F^{rep}[\rho]$ corresponding to the hard sphere is also unknown, one proceeds by making a further approximation for $F^{rep}[\rho]$. There are many different approximations for the calculation of the repulsive contribution $F^{rep}[\rho]$. Among these approximations, it is well known that the weighted-density approximations describe the structural properties of hard-sphere fluid well. Thus, the HWDA and GHWDA have been used for the calculation of the repulsive contribution $F^{rep}[\rho]$.

For the attractive contribution $F^{att}[\rho]$, there are two well known perturbation theories [8, 9], which are the density-functional mean-field approximation (DFMFT) based on the mean-field theory, and the density-functional perturbation theory (DFPT) in which is combined the nonlocal density-functional model of an inhomogeneous hard-sphere system with the Barker–Henderson second-order perturbation theory [15] of uniform simple fluids. The latter originally comes from applying to the inhomogeneous fluids the so-called macroscopic compressibility approximation, which was suggested by Barker and Henderson [15]. This approach partially incorporates the effects of potential fluctuation caused by the attractive interaction between fluid particles, so all particles are forced to move into energetically favourable positions under the constraint of hard-core exclusion. These

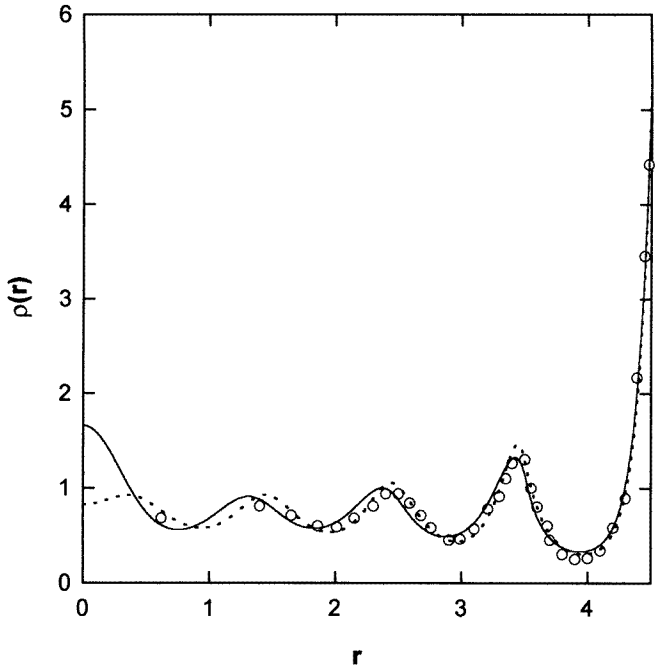


**Figure 2.** As figure 1, except that $\rho_b\sigma^3 = 0.75$.

perturbation theories have been examined by many authors [8, 9, 10] in investigating the density profiles of Lennard-Jones fluid confined in structureless hard walls and spherical cages. Notice here that Sambroski *et al* [9] have used the DFMFT theory to study the structural behaviour of Lennard-Jones fluid confined in spherical cages. They have shown that over a wide range of fluid densities the DFPT is better than the DFMFT and comparable with the computer simulations. Thus, we have here introduced the DFPT to study the density profiles of Lennard-Jones fluid confined in spherical walls. In the DFPT, the attractive term $F^{att}[\rho]$ is assumed to be

$$F^{att}[\rho] = \tfrac{1}{2}\int \mathrm{d}\boldsymbol{r}\,\rho(\boldsymbol{r})\int \mathrm{d}\boldsymbol{s}\,\rho(\boldsymbol{s})g^{hs}(\boldsymbol{r}-\boldsymbol{s};\bar{\rho})u^{att}(\boldsymbol{r}-\boldsymbol{s}) - \frac{\beta}{4}\int \mathrm{d}\boldsymbol{r}\,\rho(\boldsymbol{r})\int \mathrm{d}\boldsymbol{s}\,\rho(\boldsymbol{s})g^{hs}(\boldsymbol{r}-\boldsymbol{s};\bar{\rho})\alpha(\bar{\rho})[u^{att}(\boldsymbol{r}-\boldsymbol{s})]^2 \tag{12}$$

where $\bar{\rho} = \rho[(\boldsymbol{r}+\boldsymbol{s})/2]$ and $g^{hs}(\boldsymbol{r}-\boldsymbol{s};\bar{\rho})$ is the pair correlation function of hard-sphere fluid with the density $\bar{\rho}$. In the uniform fluids, equation (12) reduces to the Barker–Henderson second-order perturbation theory. The quality $\alpha(\rho)$ is taken to be the compressibility of hard-sphere fluid as follows:

$$\alpha(\rho) = \frac{1}{\beta}\left(\frac{\partial\rho}{\partial P}\right)^{hs} = \frac{(1-\eta)^4}{1+4\eta+4\eta^2-4\eta^3+\eta^4} \tag{13}$$

where $\eta = \pi\rho d^3/6$, $P$ is the pressure of hard-sphere fluid, and $d$ is the equivalent hard-sphere diameter. The Barker–Henderson criterion (see [16]) is used to determine the equivalent hard-sphere diameter $d$:

$$d = \int \mathrm{d}r\,[1-\exp(-\beta u^{rep}(r))] \tag{14}$$

where $d$ depends on the temperature but not on the density. From equations (2) and (9), we can easily obtain the one-particle direct correlation functions for the attractive contribution; $c^{(1)}(\boldsymbol{r};[\rho])^{att}$ and $c^{(1)}(\rho)^{att}$. For the $c^{(1)}(\boldsymbol{r};[\rho])^{att}$

$$c^{(1)}(\boldsymbol{r};[\rho])^{att} = -\int \mathrm{d}\boldsymbol{s}\,\rho(\boldsymbol{s})u^{att}(\boldsymbol{r}-\boldsymbol{s}) + \frac{\beta}{2}\int \mathrm{d}\boldsymbol{s}\,\rho(\boldsymbol{s})g^{hs}(\boldsymbol{r}-\boldsymbol{s};\bar{\rho})\alpha(\bar{\rho})[u^{att}(\boldsymbol{r}-\boldsymbol{s})]^2 \tag{15}$$

and for the $c^{(1)}(\rho_b)^{att}$

$$c^{(1)}(\rho_b)^{att} = -\rho_b\int \mathrm{d}\boldsymbol{s}\,u^{att}(\boldsymbol{r}-\boldsymbol{s}) + \frac{\beta}{2}\rho_b\int \mathrm{d}\boldsymbol{s}\,g^{hs}(\boldsymbol{r}-\boldsymbol{s};\rho_b)\alpha(\rho_b)[u^{att}(\boldsymbol{r}-\boldsymbol{s})]^2. \tag{16}$$

Then, the resulting density profile equation for the Lennard-Jones fluid is given by

$$\rho(r) = \begin{cases} \rho_b \exp[c^{(1)}(r;[\rho])^{rep} + c^{(1)}(r;[\rho])^{att} - c^{(1)}(\rho_b)^{rep} - c^{(1)}(\rho_b)^{att}] & r < R \\ 0 & r > R \end{cases} \tag{17}$$

where $c^{(1)}(r;[\rho])^{rep}$ and $c^{(1)}(\rho_b)^{rep}$ represent repulsive contributions and are given by equations (3) and (4). The density profiles are obtained by the numerical iteration between the old density profiles on the right-hand side and the new one on the left-hand side in equation (17).

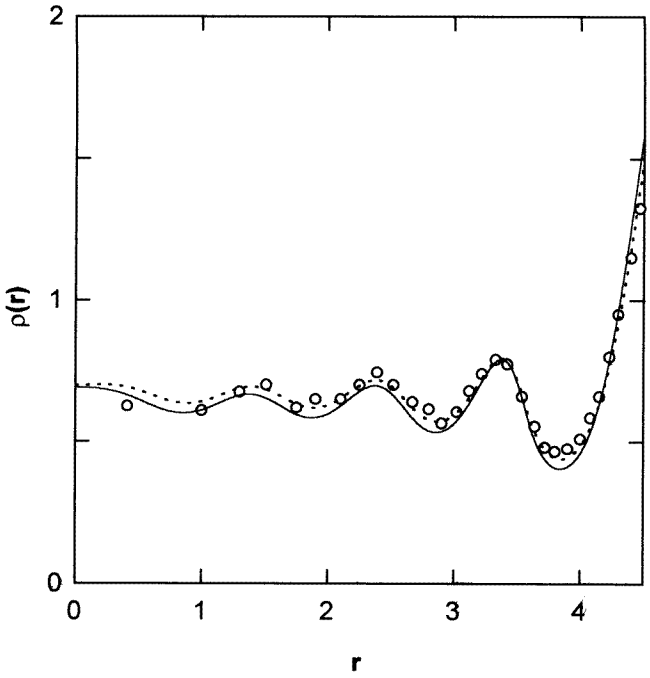


**Figure 3.** Density profiles of Lennard-Jones fluid confined in a spherical cage at the reduced temperature of 2.719. The open circles are from the computer simulations [7]. The solid and dotted lines correspond to the HWDA and GHWDA, respectively.

The resulting density profiles for the confined Lennard-Jones fluid are displayed in figures 3, 4 and 5, and compared with the computer simulations [7]. In these plots the

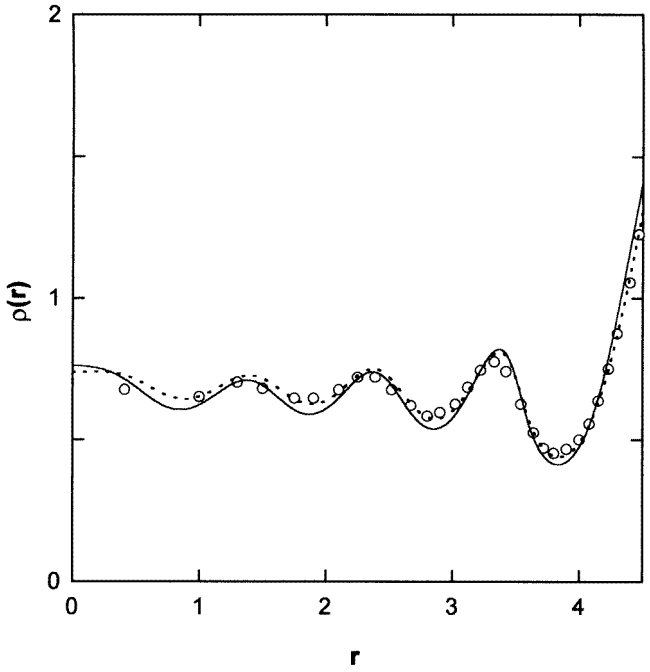


**Figure 4.** As figure 3, but with $T = 1.953$.

length, volume, and temperature are measured in units of $\sigma$, $\sigma^3$, and $\epsilon/k_B$, respectively. In terms of these units, the critical point for the DFPT is $T_c = 1.303$ and $\rho_c = 0.275$, whereas for the computer simulations $T_c = 1.36$ and $\rho_c = 0.36$. The Verlet–Weis approximation (see [17, 18]) has been used to calculate the hard-sphere pair correlation function $g^{hs}(r, \rho)$ appearing in equations (15) and (16). Through these calculations, the total number of particles in the pore, $N = 266$, is kept as a constant to compare with the computer simulations:

$$N = 4\pi \int_0^R \mathrm{d}r\, r^2 \rho(r). \tag{18}$$

As can be seen from figure 3, the DFPT at the reduced temperature $T = 2.714$ compares with the computer simulations. The results at the temperature of 1.953 are shown in figure 4. These results also show that the DFPT compares with the computer simulations. Figures 3 and 4 lead to the conclusion that at a temperature higher than the critical temperature the DFPT shows reasonably good agreement with the computer simulations. Figure 5 shows the density profiles at the temperature of 1.19—lower than the critical temperature of 1.36. At temperatures lower than the critical temperature the DFPT also shows reasonably good agreements with the computer simulations, although agreement deteriorates slightly as the temperature of Lennard-Jones fluid is reduced. However, the overall picture demonstrates that both the HWDA and GHWDA and the DFPT successfully describe the inhomogeneous properties of Lennard-Jones fluid confined in spherical cages.

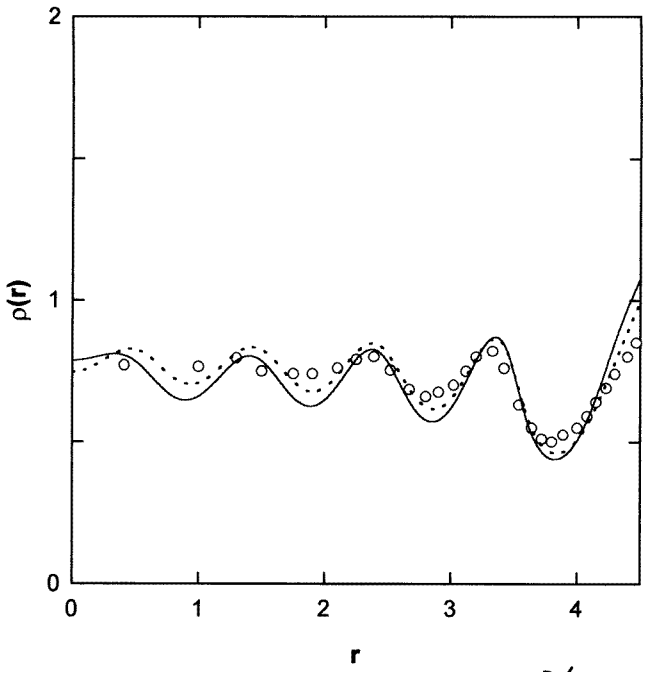


**Figure 5.** As figure 3, but with $T = 1.19$.

## 4. Results and discussion

Two different free-energy functional approximations, the HWDA and GHWDA, have been applied in the study of the density profiles of hard-sphere and Lennard-Jones fluids confined in spherical cages. Unlike for the density profiles of hard-sphere fluids restricted by permeable walls [1, 6], for the density profiles of hard-sphere fluid confined in spherical cages the GHWDA results show better agreement than the HWDA results, and compare with the computer simulations. Here, the interesting thing is that at higher density the HWDA does not describe correctly the physical behaviour of hard-sphere fluid near the centre of a spherical cage. For the Lennard-Jones fluid, the DFPT compares well with the computer simulations although the agreement deteriorates slightly as the temperature of Lennard-Jones fluid is reduced. However, the overall picture demonstrates that both the HWDA and the GHWDA and the DFPT successfully describe inhomogeneous properties of Lennard-Jones fluid, although the GHWDA is in closer agreement with the computer simulations than the HWDA. From the various applications as well as for the fluids restricted by hard and permeable walls we can conclude that the structural properties of fluids depend on the geometrical features of walls as well as the wall potentials.

On the other hand, the free-energy functional approximation presented here can be applied to the liquid–solid freezing transition of other systems such as Lennard-Jones fluid; such systems with soft repulsions are notoriously difficult to study as regards freezing transitions and constitute a stern test for any theory [19, 20]. Therefore, we intend to use the proposed HWDA and GHWDA to study the freezing problem of classical fluids. We hope to investigate these problems in the near future.

**Acknowledgments**

The author would like to thank Professor Rickayzen for helpful discussions. This work was supported by the Basic Science Research Institute Programme, Ministry of Education, 1995, project No BSRI-95-2405.

**References**

[1] Kim S C, Calleja M and Rickayzen G 1995 *J. Phys.: Condens. Matter* **7** 8053
[2] Tarazona P 1985 *Phys. Rev.* A **31** 2672; **32** 148
[3] Tarazona P, Bettolo Marconi U M and Evans R 1987 *Mol. Phys.* **60** 573
[4] Curtin W A and Ashcroft N W 1985 *Phys. Rev.* A **32** 2909
[5] Leidl R and Wagner H 1993 *J. Chem. Phys.* **98** 4142
[6] Kim S C, Calleja M and Rickayzen G 1995 unpublished
[7] Calleja M, North A N, Powles J G and Rickayzen G 1991 *Mol. Phys.* **73** 973
[8] Tang Z, Scriven L E and Davis H T 1991 *J. Chem. Phys.* **95** 2659
[9] Sambroski A, Stecki J and Poniewierski A 1993 *J. Chem. Phys.* **98** 8958
[10] Henderson D and Sokolowski S 1995 *Phys. Rev.* E **52** 758
[11] Carnahan N F and Starling K E 1969 *J. Chem. Phys.* **51** 635; 1970 *J. Chem. Phys.* **53** 600
[12] Kim S C, Suh J K and Suh S H 1993 *Mol. Phys.* **79** 1369
[13] Chui S T 1990 *Phys. Rev.* B **43** 10 654
[14] Evans R 1979 *Adv. Phys.* **28** 143
[15] Barker J S and Henderson D 1976 *Rev. Mod. Phys.* **48** 587
[16] Hansen J P and McDonald I R 1986 *Theory of Simple Liquids* 2nd edn (New York: Academic)
[17] Verlet L and Weis J J 1972 *Phys. Rev.* A **5** 939
[18] McQuarrie D A 1973 *Statistical Mechanics* (New York: Harper and Row)
[19] Singh Y 1991 *Phys. Rep.* **207** 351
[20] Löwen H 1994 *Phys. Rep.* **237** 249